

NASA-CR-194525

0017

187810

21P

Vacuum Ultraviolet Instrumentation for Solar Irradiance  
and Thermospheric Airglow

Thomas N. Woods and Gary J. Rottman

High Altitude Observatory  
National Center for Atmospheric Research

Boulder, Colorado 80307-3000

Phone: 303-497-1574

FAX: 303-497-1589

E-Mail: woods@virgo.hao.ucar.edu

rottman@virgo.hao.ucar.edu

Scott M. Bailey and Stanley C. Solomon

Laboratory for Atmospheric and Space Physics

University of Colorado

1234 Innovation Drive, Boulder, Colorado 80303

Phone: 303-492-0457

FAX: 303-492-6444

E-Mail: bailey@virgo.hao.ucar.edu

solomon@tethys.colorado.edu

N94-14684

Unclas

G3/35 0187810

*Optical Engineering*

8/25/93

(NASA-CR-194525) VACUUM  
ULTRAVIOLET INSTRUMENTATION FOR  
SOLAR IRRADIANCE AND THERMOSPHERIC  
AIRGLOW Semiannual Report, FY 1993  
(National Center for Atmospheric  
Research) 21 p

## ABSTRACT

A NASA sounding rocket experiment was developed to study the solar extreme ultraviolet (EUV) spectral irradiance and its effect on the upper atmosphere. Both the solar flux and the terrestrial molecular nitrogen via the Lyman-Birge-Hopfield bands in the far ultraviolet (FUV) were measured remotely from a sounding rocket on October 27, 1992. The rocket experiment also includes EUV instruments from Boston University (Supriya Chakrabarti), but only the National Center for Atmospheric Research (NCAR) / University of Colorado (CU) four solar instruments and one airglow instrument are discussed here. The primary solar EUV instrument is a 1/4 meter Rowland circle EUV spectrograph which has flown on three rockets since 1988 measuring the solar spectral irradiance from 30 to 110 nm with 0.2 nm resolution. Another solar irradiance instrument is an array of six silicon XUV photodiodes, each having different metallic filters coated directly on the photodiodes. This photodiode system provides a spectral coverage from 0.1 to 80 nm with about 15 nm resolution. The other solar irradiance instrument is a silicon avalanche photodiode coupled with pulse height analyzer electronics. This avalanche photodiode package measures the XUV photon energy providing a solar spectrum from 50 to 12,400 eV (25 to 0.1 nm) with an energy resolution of about 50 eV. The fourth solar instrument is an XUV imager that images the sun at 17.5 nm with a spatial resolution of 20 arc-seconds. The airglow spectrograph measures the terrestrial FUV airglow emissions along the horizon from 125 to 160 nm with 0.2 nm spectral resolution. The photon-counting CODACON detectors are used for three of these instruments and consist of coded arrays of anodes behind microchannel plates. The one-dimensional and two-dimensional CODACON detectors were developed at CU by Dr. George Lawrence. The pre-flight and post-flight photometric calibrations were performed at our calibration laboratory and at the Synchrotron Ultraviolet Radiation Facility (SURF) at the National Institute of Standards and Technology (NIST) in Gaithersburg, Maryland.

## 1. SCIENTIFIC OBJECTIVES

The primary objectives of this investigation are the comparison of results from various solar extreme ultraviolet (EUV) instruments suitable for long-term satellite missions and the calibration of the solar-photoelectron relationship as derived with simultaneous solar and airglow measurements. We will use the general EUV term to mean the classical extreme ultraviolet from 20 to 120 nm and the XUV (soft x-ray, EUV) from 0.1 to 20 nm. Due to the lack of recent data on the solar EUV irradiance, the solar cycle variation of fluxes in the EUV region of the solar spectrum are not well understood. However, the solar EUV flux is of crucial importance to several topics in the physics of the ionosphere, thermosphere, mesosphere, and stratosphere because this broad range of solar EUV radiation is mostly deposited in the upper atmosphere providing the heat and energy to form the ionosphere and to control the dynamics of the thermosphere. For this investigation, we continue to provide this fundamental measurement of the full-disk solar EUV spectral irradiance during solar cycle 22 and compare measurements from four different solar EUV instruments in a single sounding rocket payload. These different simultaneous solar measurements cover the spectral range from 0.1 to 120 nm with various spectral resolutions from 0.2 to 15 nm, and they help clarify the suitability of these instruments for long-term satellite missions. In addition, simultaneous far ultraviolet (FUV) airglow measurements with high spectral resolution are obtained to study the solar-photoelectron relationship using the molecular nitrogen Lyman-Birge-Hopfield (LBH) bands and the atomic oxygen lines at 130.4 and 135.6 nm. Because the atmospheric densities of the neutral species can be derived by measuring the absorption of the solar flux as a function of wavelength and altitude, the models of photoelectron impact processes in the Earth's atmosphere, such as the emission of the N<sub>2</sub> LBH bands, can be unambiguously validated and verified. Thus, the airglow measurements enhance the usefulness of the FUV airglow emissions for thermospheric remote sensing by spacecraft. This rocket payload was launched on a "World Day", on October 27, 1992, to enhance the data set and results from many coordinated upper atmosphere experiments.

The solar EUV flux has been measured by sounding rocket and satellite instruments for more than two decades, mainly by the Air Force Cambridge Research Laboratories (AFCRL) [Orbiting Solar Observatory 3 (OSO-3)<sup>1</sup>; series of Atmospheric Explorers (AE-C,D,E)<sup>2</sup>]. The most commonly used reference solar EUV flux for atmospheric modeling (i.e. calculating typical photoelectrons, heating, etc.) is the revised AE-E data representative for the solar minimum and maximum conditions during solar cycle 21<sup>3,4</sup>. The calibration of the revised AE-E data set is based on sounding rocket measurements because there were no provisions for in-flight calibrations of the instrument on AE-E<sup>3</sup>. These previous results have been in controversy over the total solar cycle variation<sup>5,6</sup>, discrepancies in the absolute flux due to the AE-E instrument degradation and the use of several different instruments<sup>3,7,8</sup>. After solar cycle 20, Heroux and Higgins<sup>7</sup> concluded that the solar EUV flux varied by about 10% over a solar cycle from six different rocket measurements; whereas, the revised AE-E solar EUV flux varies by a factor of 3 over solar cycle 21. A more recent estimate of the solar UV flux variability at Lyman  $\alpha$  is 60% from the SME data<sup>8</sup>. These estimates for the solar flux variations are for the bright chromospheric emissions as the weaker corona emissions vary more wildly by a few orders of magnitude during a solar cycle. Following the last AE-E measurements in 1980, there has been a long hiatus with only a few measurements of the solar EUV flux, and appropriately Donnelly<sup>9</sup> refers to this lack of current solar EUV spectral irradiance measurements as the "solar EUV hole".

The recent solar EUV spectral irradiance observations include those from the San Marco 5 satellite in 1988 and a couple of sounding rocket measurements<sup>10</sup>. The recent solar VUV irradiance measurement on October 27, 1992 is shown in figure 1. The controversial solar EUV flux, especially at the shorter wavelengths, needs to be measured accurately for both the upper atmospheric and solar physicists. This experiment package directly addresses the absolute magnitude of the solar spectral flux at the shorter XUV wavelengths as well as the EUV spectral region and provides simultaneous observations with different types of solar EUV instruments in

order to resolve any discrepancies related to instrument behavior and calibration. Because the atmospheric cross section for the solar radiation has a continuum shape below 60 nm, it is not necessary to have spectral resolution better than a few nm in order to address the magnitude of the solar XUV flux at the shorter wavelengths. Consequently, this rocket experiment has solar instruments with low spectral resolution plus one higher resolution spectrograph to cover the solar spectrum at the longer wavelengths with the desired resolution of about 0.2 nm.

The central problem of airglow analysis in the sunlit thermosphere is the relationship of solar fluxes to emission features. The solar flux from the visible to the far ultraviolet and laboratory cross sections are known well enough so that most resonance and fluorescence processes are no longer uncertain to any great degree. However, solar EUV fluxes are still the greatest single free parameter in the analysis of photoionization and photoelectron excited emissions. Attempts to reconcile the solar flux with the photoelectron flux have suggested that the solar flux at the shorter wavelengths (less than 25 nm) from solar models such as Hinteregger *et al.*<sup>3</sup> are insufficient to produce measured photoelectron fluxes at both low and high solar activity<sup>11,12</sup>.

In order to establish the solar-photoelectron relationship, emission bands which respond directly to photoelectron excitation without complications of chemical reactions are preferred. An example of this is the N<sub>2</sub> second positive band system. The N<sub>2</sub> second positive band system is forbidden in absorption (C - X) but permitted in emission (C - B). The N<sub>2</sub> LBH band system is marginally forbidden and hence does not fluoresce but emits fast enough to avoid chemical deactivation above about 100 km. Figure 1 shows a model spectrum of the LBH bands as would be seen from a rocket viewing horizontally during high solar activity. Past studies of FUV emissions have used LBH bands to calibrate photoelectron fluxes<sup>13,14</sup> which may then be used in the analysis of OI emissions. Cross-sections for electron impact excitation<sup>15</sup> are relatively well established for the LBH system, as are the complicating factors of absorption by O<sub>2</sub> and self absorption of the  $v''=0$  transitions<sup>16</sup>. However, the lack of simultaneous measurements of solar

fluxes and atmospheric densities introduce serious uncertainties. Past practice has been to adjust the solar flux or photoelectron flux to reproduce the LBH measurements, under a particular assumption concerning N<sub>2</sub> densities, and then use this parameterization to model the more difficult OI emissions.

Modeling the LBH bands will be based on all the relevant inputs, and not adjustable parameters, thus allowing close examination of cross-sections and model validity. The measured inputs include the solar fluxes at all the important wavelengths, and the neutral densities derived from the atmospheric attenuation of the solar flux. Photoelectron codes for analysis of these emissions have been developed<sup>17,18</sup>, so the tools for detailed comparison of model and data are at hand. Measurement of the LBH bands as a means of establishing the photoelectron flux is a primary goal of the airglow experiment. The instrument is optimized for this, with sufficient sensitivity and spectral resolution to investigate all significant emission features. In addition, the atomic oxygen lines at 130.4 and 135.6 and the atomic nitrogen line at 149.3 nm are observed and used to confirm our knowledge of the neutral atmosphere. The neutral atmosphere is also determined empirically from the amount of attenuation of the solar EUV radiation as the rocket ascends and descends through the atmosphere.

## 2. EUV SOLAR IRRADIANCE EXPERIMENT

The EUV Solar Irradiance Experiment (ESIE) consists of a 1/4 m (EUV) spectrograph for obtaining full-disk solar irradiance. The optical layout of this instrument is shown in figure 2. The 1/4 m spectrograph is a normal-incidence Rowland circle spectrograph with a 1 x 1024 CODACON array detector. It has a spectral coverage of 25 to 120 nm with a 0.1 nm bandpass per anode on the detector, and an overall spectral resolution of about 0.3 nm. The concave diffraction grating is a tripartite grating with a ruling density of 1028 lines/mm. The grating is gold coated for increased reflectivity in the EUV. A complete solar spectrum is possible in less than 1 second due

to the use of an array detector; therefore, atmospheric absorption information at all wavelengths is available on  $\approx 1$  km intervals. The CODACON array detector is described later. This spectrograph has been flown three times since 1988, and some of those results are described in more detail by Woods and Rottman<sup>10</sup>.

### 3. XUV PHOTOMETERS

A package of six silicon photodiodes is used to measure the EUV and XUV irradiance with approximately 15 nm resolution. Ogawa *et al.*<sup>19</sup> flew a photodiode of this type with an aluminum filter and were able to obtain the integrated EUV irradiance from 17 to 80 nm. This experiment improves upon their measurement in three ways. First the thin film filters are coated directly on the photodiode and no thin foil filters are used. This simplifies and stabilizes the photometer as the metal foils are difficult to handle, prone to develop pin holes and degrade with time. The second improvement is the use of multiple photodiodes with different filters to achieve a low resolution XUV spectrum. The third enhancement is to extend the measurement below 17 nm.

The XUV photodiodes used are commercially available and have been described by Korde and Geist<sup>20</sup> and Korde *et al.*<sup>21</sup>. Sensitivity and stability measurements have also been published by Husk *et al.*<sup>22</sup>, Canfield *et al.*<sup>23</sup>, Korde and Canfield<sup>24</sup> and Korde *et al.*<sup>21</sup>. Typical sensitivities are about one electron per photon for a 10 eV photon and 24 electrons per photon for a 100 eV photon. Korde and Canfield<sup>23</sup> report stability to within a percent after exposure to  $10^{14}$  photons/cm<sup>2</sup> at 124 eV and no noticeable change in quantum efficiency after several months of storage at room temperature. These diodes have been adopted by the National Institute for Standards and Technology as one of their standard XUV detectors.

There are several suitable metals for use as filters and the use of multiple coatings on the same diode provides a way of narrowing the bandpass of each diode. Powell *et al.*<sup>25</sup> discusses the

current state of the art for filters in this wavelength range. We use a combination of the following materials to achieve low resolution bandpass filters: aluminum, titanium, beryllium, carbon, tin and indium.

As shown in figure 3 the XUV photodiodes are used with voltage-to-frequency converter electronics to accurately measure their current. Typical currents for the solar XUV irradiance are expected at the level of 1-100 nA and are dependent on wavelength range and area of their aperture. The typical background current for these photodiodes is usually 0.01 to 0.1 nA.

#### 4. ADVANCED X-RAY SPECTROMETER

The Advanced X-ray Spectrometer (AXS) consists of a silicon avalanche photodiode and pulse height analyzer electronics and is shown in figure 3. The AXS is used in photon counting mode by using the modest gains of about 100 for the avalanche photodiode coupled with the generation of many electrons for a single XUV photon ( $1 e^-$  per 3.63 eV of photon energy). The pulse height analyzer electronics use state-of-the-art charge amplifiers capable of resolving better than 1,000 electrons; therefore, the limitations on the upper wavelength for the AXS is primarily the thermal noise of the avalanche photodiode. The lower wavelength limit is about 0.01 nm related to the higher transmission of silicon at the shorter wavelengths. The avalanche photodiode has a thin aluminum passivation layer for stability reasons for the silicon interface and a thicker titanium coating to make the device "solar blind". The AXS is designed to measure the XUV photon energy from 50 to 12,400 eV (25 to 0.1 nm) with a energy resolution of about 50 eV.

A set of six XUV photodiodes and one avalanche photodiode is packaged together with a common shutter door. There are MgF<sub>2</sub> windows for each diode on this door to permit accurate subtraction of the background signal, if any from visible and FUV light. The background signal is measured at the beginning, middle and end of the solar measurements when the shutter door is



closed.

## 5. XUV IMAGER

The XUV Imager, as shown in figure 4, consists of a two dimensional CODACON detector with a telescope mirror and two aluminum/lexan foil filters in front of the detector. The detector array has 256 x 256 anodes with each anode being 38  $\mu$  x 38  $\mu$ . A multilayer dielectric coating on the mirror<sup>26</sup> and the aluminum/lexan filter combine for a 1 nm wide bandpass at 17.7 nm; thus, the solar iron lines at  $1-2 \times 10^6$  °K in the corona are the primary contributions to the solar XUV image. A vacuum door is mounted to the CODACON detector housing to keep the detector evacuated / clean and to protect the foil filters from acoustical vibrations during launch. The concave telescope mirror has a focal length of 750 mm. The instrument has a field of view of 44 arc-minutes and spatial resolution of 10 arc-seconds. This imager flew on a rocket in 1992 and 1989<sup>27</sup> as well as a similar version using a 128 x 128 CODACON<sup>28</sup> which flew on a rocket in 1988. Images have been made continuously throughout the previous flights with each unique image possible after integrating for several seconds.

## 6. FUV AIRGLOW SPECTROGRAPH

The FUV Airglow spectrograph consists of a Wadsworth grating configuration, a telescope and a 1 x 1024 CODACON detector and is shown in figure 5. The telescope is an  $f/2$  CaF<sub>2</sub> plano-convex lens. The transmission function of CaF<sub>2</sub> is fortuitous in this application because its throughput is low at 130 nm and increases rapidly above 140 nm. Thus the bright atomic oxygen emissions at 130.4 and 135.6 emissions are prevented from saturating the detector, while the dimmer LBH emissions at longer wavelengths are not severely affected.

The Wadsworth mount consists of an off-axis parabolic mirror and a concave grating. The

parabolic mirror is  $f/2$  with a focal length of 152 mm. The concave grating has a 600 mm radius of curvature and a ruling density of 2083 lines/mm. The instrument covers the wavelength range from 125.0 to 160.0 nm with a resolution of 0.2 nm.

Altitude resolution is determined by the field of view of the telescope, observing conditions and the velocity of the rocket. At altitudes where count rates are low, data is summed along altitude to obtain better counting statistics at the price of lower altitude resolution. Based on observing conditions and typical rocket velocities (on the order of 1 km/s), we get an altitude resolution of 10 to 15 km depending on wavelength and altitude.

## 7. CODACON ARRAY DETECTOR

The detector used for three of the rocket instruments is the photon-counting CODACON array detector which was developed by Dr. George Lawrence at the University of Colorado<sup>29</sup>. Both the one-dimensional and two-dimensional versions of the CODACON detector have flown numerous times on previous sounding rocket payloads. These detectors consist of a microchannel plate (MCP) and a multi-anode "code plate". When a photon releases an electron from the photocathode on top of the MCP, the MCP amplifies this electron with a gain of about  $10^6$ . These packets of electrons impinge on the anodes which are coded to have  $n$  bits where  $2^n$  equals the total number of anodes along one axis. Because the signal from each anode is activated by the capacitance between a large anode and a coded anode array, there are two charge amplifiers per bit. Thus, only 20 charge amplifiers are required for the  $1 \times 1024$  CODACON, and 32 amplifiers are needed for the  $256 \times 256$  CODACON detector. The coded anode data, being  $n$  bits of information, is either accumulated by a memory board for making a spectrum or stored in a FIFO (first in first out) circuit for buffering single photon events. The ESIE and airglow spectrographs use a  $1 \times 1024$  CODACON and the XUV imager employs a  $256 \times 256$  CODACON detector.

## 8. CALIBRATIONS

The four solar instruments are calibrated at the Synchrotron Ultraviolet Radiation Facility (SURF) at the National Institute of Standards and Technology (NIST) in Gaithersburg, Maryland. Typical uncertainties for this type of calibration are about 5-10%<sup>10</sup>. For the 1/4 meter spectrograph (ESIE) multiple SURF beam energies are used to derive the contribution from different diffraction orders of the grating<sup>10,30</sup>. The XUV photometer's sensitivity as a function of wavelength is obtained at NIST using a grazing incidence monochromator with the SURF beam. This monochromator system is calibrated in the range 5 to 100 nm so that a signal of known wavelength and intensity is incident on the photometer. Current measurements as a function of wavelength then yield a sensitivity calibration. This part of the calibration is performed by L. Randall Canfield of NIST. The components of the XUV Imager, the CODACON detector, foil filters and telescope mirror are calibrated separately at SURF.

The airglow spectrograph is calibrated using the HAO/NCAR vacuum calibration facility. The calibration facility is equipped with platinum and deuterium lamps as emission line sources, a UV monochromator with a  $f/80$  output beam for selecting single emission lines, and a reference detector traceable to NIST standards for determining the absolute flux from the selected emission line. Quantum throughput (QT) measurements for the telescope and spectrograph, without its entrance slit installed, are made separately. This provides a QT of the instrument at the center of the field of view (FOV). The instrument is then reassembled and pointed at a scattering screen. Spectra are then taken with the FOV filled and with the telescope masked to only partially fill the optics. The ratio of these two measurements provides the effect of filling the optics compared to a calibration at the center of the FOV. The final quantum throughput of the instrument is the product of the ratio of the scattering screen measurements, the QT of the telescope and the QT of the instrument measured at the center of the FOV.

## 9. FLIGHT CONFIGURATION

The payload is an aft-looking Terrier-Black Brant rocket with a three-axis-controlled solar-pointing Altitude Control System (ACS). We use the Lockheed Solar ACS called the Solar Pointing Attitude Rocket Control System (SPARCS) because it is a versatile system with which we have had great success over the last several years. All of these instruments had a successful rocket flight from the White Sands Missile Range (WSMR) in New Mexico on October 27, 1992. A launch time near local noon minimized the atmospheric absorption for the solar measurements.

The payload configuration, shown in figure 6 for the scientific instruments, includes a vacuum section for the solar instruments, a section for the airglow spectrograph and an electronics section. The Boston University instruments are housed in half of the solar section (PI: S. Chakrabarti). The solar section is evacuated for the windowless microchannel plate detectors. The other payload sections contain the standard telemetry, ACS, recovery and separation subsystems provided by NASA (contracts to White Sands Missile Range (WSMR) Lockheed in this case).

Because the solar instruments are aft-looking, the payload maneuvers up about  $180^\circ$  near the beginning of the flight to track the sun during the remaining part of the controlled flight. The airglow instrument looks east and horizontally with a constant zenith angle between  $80^\circ$  and  $90^\circ$ . Because the solar zenith angle at local noon slowly changes throughout the year, the airglow spectrograph is designed to rotate in its mounting frame to permit a rocket launch at anytime during the year. The solar EUV spectral irradiance measurements from 0.1 to 120 nm and the airglow FUV measurements from 125 to 160 nm are made from about 200 km on the up-leg portion of the flight until about 100 km on the down-leg portion of the flight. The apogee of the flight is about 300 km.

## 10. ACKNOWLEDGMENTS

This research effort is supported by NASA grant NAG5-676. We are grateful to the payload design/operations team at the National Center for Atmospheric Research and the University of Colorado including Rick Kohnert, Greg Ucker, Kip Denhalter and Ray Wrigley along with many other supporting engineers and technicians. We also thank the NASA Wallops Flight Center and WSMR Lockheed personnel for their support of this rocket experiment.

## 11. REFERENCES

1. L. A. Hall and H. E. Hinteregger, "Solar Radiation in the Extreme Ultraviolet and its Variation with Solar Rotation", *J. Geophys. Res.*, **75**, 6959 (1970).
2. H. E. Hinteregger, K. Fukui, and B. R. Gilson, "Observational, Reference and Model Data on Solar EUV from Measurements on AE-E", *Geophys. Res. Letters*, **8**, 1147 (1981).
3. H. E. Hinteregger, D. E. Bedo, and J. E. Manson, "The EUV Spectrophotometer on Atmosphere Explorer", *Radio Science*, **8**, 349 (1973).
4. M. R. Torr and D. G. Torr, "Ionization Frequencies for Solar Cycle 21: Revised", *J. Geophys. Res.*, **90**, 6675 (1985).
5. R. G. Roble, "Solar EUV Variation During a Solar Cycle as Derived from Ionospheric Modeling Considerations", *J. Geophys. Res.*, **81**, 265 (1976).
6. L. Oster, "Solar Irradiance Variations, 2. Analysis of the Extreme Ultraviolet Spectrometer Measurements Onboard the Atmospheric Explorer E satellite", *J. Geophys. Res.*, **88**, 9037 (1983).
7. L. Heroux and J. E. Higgins, "Summary of Full-disk Solar Fluxes Between 250 and 1940 Å", *J. Geophys. Res.*, **82**, 3307 (1977).
8. G. J. Rottman, "Results from Space Measurements of Solar UV and EUV Flux", *Solar Radiative Output Variation*, P. Foukal (Ed.), Cambridge Research and Instrumentation Inc, Boulder, CO, 71 (1987).
9. R. F. Donnelly, "Gaps Between Solar UV & EUV Radiometry and Atmospheric Sciences",

*Solar Radiative Output Variation*, P. Foukal (Ed.), Cambridge Research and Instrumentation Inc, Boulder, CO, 139 (1987).

10. T. N. Woods and G. J. Rottman, "Solar EUV Irradiance Derived from a Sounding Rocket Experiment on 10 November 1988", *J. Geophys. Res.*, **95**, 6227 (1990).

11. P. G. Richards and D. G. Torr, "Ratios of Photoelectron to EUV Ionization Rates for Aeronomic Studies", *J. Geophys. Res.*, **93**, 4060 (1988).

12. J. D. Winningham, D. T. Decker, J. U. Kozyra, J. R. Jasperse, A. F. Nagy, "Energetic (>60 eV) Atmospheric Photoelectrons", *J. Geophys. Res.*, **94**, 15335 (1989).

13. R. W. Eastes, P. D. Feldman, E. P. Gentieu, and A. B. Christensen, "The Ultraviolet Dayglow at Solar Maximum: 1. Far UV Spectroscopy at 3.5 Å Resolution", *J. Geophys. Res.*, **90**, 6594 (1985).

14. R. R. Meier, R. R. Conway, D. E. Anderson, Jr., P. D. Feldman, R. W. Eastes, E. P. Gentieu, and A. B. Christensen, "The Ultraviolet Dayglow at Solar Maximum: 3. Photoelectron-excited Emissions of N<sub>2</sub> and O", *J. Geophys. Res.*, **90**, 6608 (1985).

15. J. M. Ajello and D. E. Shemansky, "A Reexamination of Important N<sub>2</sub> Cross Sections by Electron Impact with Application to the Dayglow: the Lyman-Birge-Hopfield Band System and NI (119.99 nm)", *J. Geophys. Res.*, **90**, 9845 (1985).

16. R. R. Conway, "Self-absorption of the N<sub>2</sub> Lyman-Birge-Hopfield Bands in the Far Ultraviolet Dayglow", *J. Geophys. Res.*, **87**, 859 (1982).

17. R. Link, S. Chakrabarti, G. R. Gladstone, and J. C. McConnell, "An Analysis of Satellite Observations of the OI EUV Dayglow", *J. Geophys. Res.*, **93**, 2693 (1988).

18. S. C. Solomon, and V. J. Abreu, "The 630 nm Dayglow", *J. Geophys. Res.*, **94**, 6817 (1989).

19. H. S. Ogawa, L. R. Canfield, D. McMullin, and D. L. Judge, "Sounding Rocket Measurement of the Absolute Solar EUV Flux Utilizing a Silicon Photodiode", *J. Geophys. Res.*, **95**, 4291 (1990).

20. R. Korde and J. Geist, "Quantum Efficiency Stability of Silicon Photodiodes", *Applied Optics*, **26**, 5284 (1987).
21. R. Korde, L. R. Canfield, and B Wallis, "Stable High Quantum Efficiency Silicon Photodiodes for Vacuum-UV Applications, *SPIE*, **932**, 153 (1988).
22. D. E. Husk, C. Tarrío, E. L. Benitez, and S. E. Schnatterly, "Response of Photodiodes in the Vacuum Ultraviolet", *J Appl. Phys.*, **70**, 6, 3338 (1991).
23. L. R. Canfield, J. Kerner and R. Korde, "Stability and Quantum Efficiency Performance of Silicon Photodiode Detectors in the Far Ultraviolet", *Applied Optics*, **28**, 3940 (1989).
24. R. Korde and L. R. Canfield, "Silicon Photodiodes with Stable, Near Theoretical Quantum Efficiency in the Soft X-ray Region", *SPIE*, **1140**, 126 (1989).
25. F. R. Powell, P. W. Vedder, J. F. Lindblom, S. F. Powell, "Thin Film Filter Performance for Extreme Ultraviolet and X-Ray Applications", *SPIE*, **26**, 9, 614 (1990).
26. B. M. Haisch, T. E. Whittemore, E. G. Joki, and W. J. Brookover, G. J. Rottman, " A Multilayer X-Ray Mirror For Solar Photometric Imaging Flown on a Sounding Rocket *SPIE*, **982**, 38 (1988).
27. M. Guhathakurta, G. J. Rottman, F. Q. Orall, and B. M. Haisch, "Sounding Rocket XUV Observations of the Corona and the Transition Region Taken on June 20 1989, *Workshop No. 3: On Max' 91/Smm Solar Flares: Observations and Theory, Estes Park, Colorado* (1990).
28. M. Guhathakurta, "The Large and Small Scale Density Structure in the Solar Corona", *Doctoral Thesis, University of Denver/LASP* (1989).
29. W. E. McClintock, C.A. Barth, R.E. Steele, G.M. Lawrence, and J.G. Timothy, "Rocket-borne Instrument with a High-resolution Microchannel Plate Detector for Planetary UV Spectroscopy", *Applied Optics*, **21**, 3071 (1982).
30. E. B. Saloman, "Unfolding First and Second Order Diffracted Radiation When Using Synchrotron Radiation Sources: A Technique", *Applied Optics*. **24**. 3206 (1985).

## FIGURE CAPTIONS

**Figure 1.** The Solar EUV Irradiance and N<sub>2</sub> LBH band system. Figure 1a is the solar spectrum obtained on October 27, 1992 is representative of moderate solar activity and is based on rocket measurements below 119 nm and on UARS SOLSTICE measurements above 119 nm. Figure 1b shows model predictions for high solar activity of the N<sub>2</sub> LBH spectrum viewed horizontally from an altitude of 150 km. Pure absorption by O<sub>2</sub> has been taken into account. Emissions by atomic oxygen and atomic nitrogen are not shown.

**Figure 2.** The EUV Solar Irradiance Experiment (ESIE). The ESIE is a 1/4 m Rowland circle spectrograph with a 1 x 1024 CODACON detector. The ESIE measures the solar EUV irradiance from 30 to 120 nm with 0.1 nm resolution per anode at the detector.

**Figure 3.** Solar XUV Photometer and Advanced X-Ray Spectrometer. The XUV photometers use a XUV silicon photodiode and voltage-to-frequency converter electronics. The Advanced X-Ray Spectrometer (AXS) uses a silicon avalanche photodiode with pulse height analyzer electronics. Six XUV photometers and one AXS is packaged together as a single subsystem having a common shutter door.

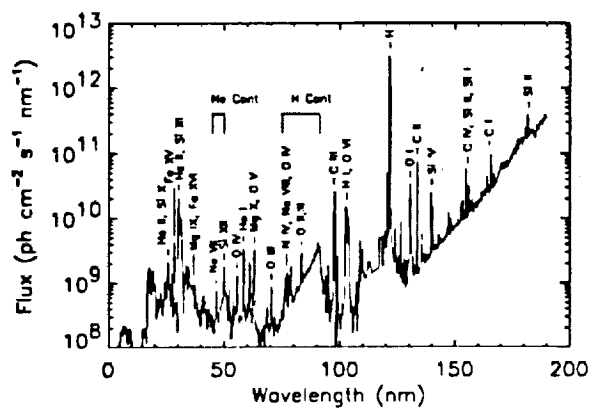
**Figure 4.** The Solar XUV Imager. The XUV Imager is a simple optical system consisting of a spherical mirror with a multilayer coating and a 256 x 256 CODACON detector with aluminum/lexan filters.

**Figure 5.** The FUV Airglow Spectrograph. The optical path is through the telescope (CaF<sub>2</sub> lens) into the Wadsworth spectrograph which consists of a off-axis parabolic collimator, a spherical diffraction grating and a 1 x 1024 CODACON detector. The spectral coverage is 127 to 170 nm with a 0.2 nm spectral resolution. The altitude resolution is about 2 to 4 km.



**Figure 6. Rocket Payload Configuration.** The solar instruments are in the upper section, the airglow spectrograph is in the middle section, and the control and power distribution electronics are in the lower section. Vacuum bulkheads separate the sections for contamination control.

(a) Solar VUV Spectrum



(b) N<sub>2</sub> LBH Emissions

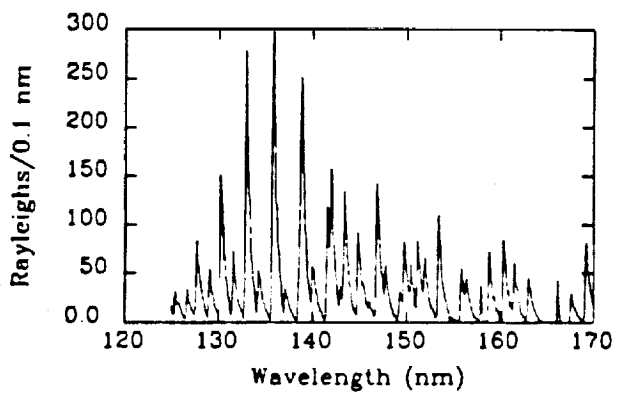


Figure 1

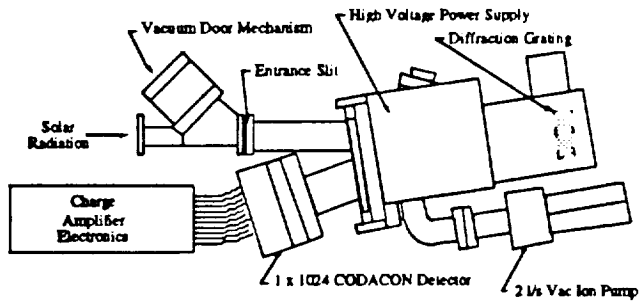


Figure 2

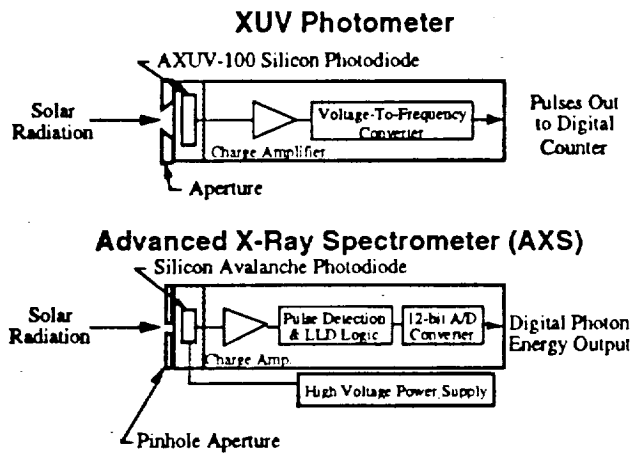


Figure 3

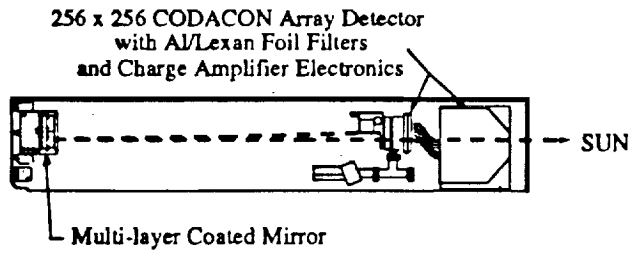


Figure 4

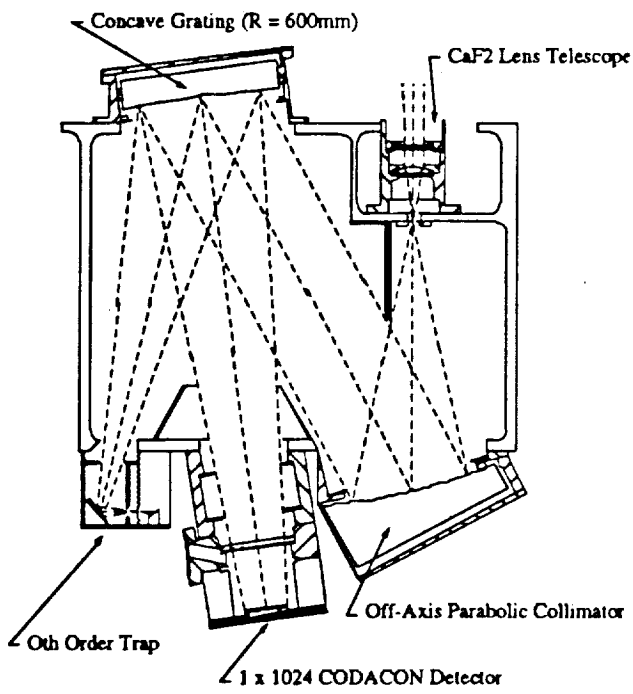


Figure 5

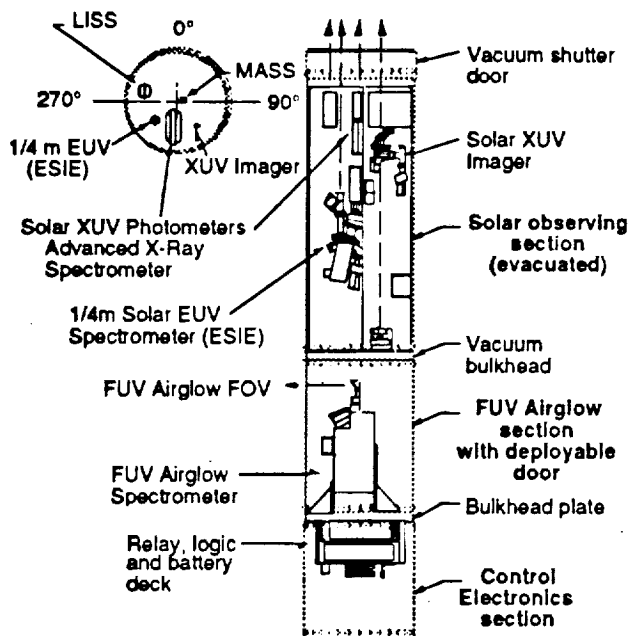


Figure 6